JOURNAL OF PROPULSION AND POWER
Vol. 26, No. 6, November–December 2010

Technical Notes

Energy-Loss Mechanisms of a Low-Discharge-Voltage Hall Thruster

Jerry L. Ross,* Jason D. Sommerville,* and Lyon B. King†
Michigan Technological University, Houghton, Michigan 49931

DOI: 10.2514/1.47777

Nomenclature

e	=	elementary charge, C
f_i	=	ionization mass fraction of the propellant
I_d	=	discharge current, A
I_i	=	exhausted ion current, A
I_{sp}	=	specific impulse, s
$j(\theta)$	=	ion current density, A/m^2
M	=	spacecraft mass, kg
m	=	mass of a xenon atom/ion, kg
$\dot{m}$	=	flow rate of propellant as determined by the mass-flow controller, kg/s
P	=	kinetic power delivered to the spacecraft, W
P_s	=	supply output power $I_d V_d$, W
Q	=	average charge state of the ionized propellant
q	=	charge number
T	=	thrust, N
U_e	=	ion velocity, m/s^2
V_{accel}	=	acceleration potential for a given ion, V
V_d	=	discharge voltage (anode potential), V
β	=	average offaxis ion trajectory angle
Δt	=	trip time, s
ΔV	=	velocity increment, m/s^2
ϵ_{ion}	=	ion kinetic energy
η_B	=	beam divergence as an efficiency
η_c	=	current efficiency
η_E	=	energy efficiency
η_p	=	propellant efficiency
η_{probe}	=	the product of all probe-measured efficiencies
η_T	=	thrust efficiency
η_v	=	voltage utilization efficiency
η_{vdf}	=	velocity distribution efficiency
θ	=	angle from thruster axis
Φ_{ctg}	=	cathode to ground potential, V
Φ_{plasma}	=	plasma to ground potential, V

I. Introduction

THE Hall thruster belongs to a class of electric propulsion that uses electric and magnetic fields to ionize and accelerate propellant. Electric spacecraft thrusters, such as the Hall thruster, can greatly decrease the propellant mass required to perform a desired mission ΔV because of their high exhaust velocities [1]. However, because the power available on spacecraft is limited to, at present, tens of kilowatts, electric propulsion devices are limited in thrust to hundreds of millinewtons. This implies that although electric propulsion can save propellant mass, it is sometimes accompanied by increased trip time for near-Earth missions. The trip time is related to the required velocity change, spacecraft mass, and thrust by

$$\Delta t = \frac{M \Delta V}{T} \tag{1}$$

The spacecraft mass M and mission ΔV are fixed quantities; hence, when the trip time is of greatest concern, a high-thrust device is required.

For an electric thruster, the relation between thrust, power, and specific impulse can be expressed as

$$T = \frac{2\eta_T P_s}{U_e} \tag{2}$$

While greater thrust can be obtained by increasing P_s, spacecraft power is limited by the on-board energy source and greater spacecraft power comes at the price of increased vehicle mass. To increase the thrust at fixed power, U_e must be decreased while maintaining a high level of η_T. The exit velocity of the ionized propellant relates to the accelerating potential according to

$$\tfrac{1}{2} m U_e^2 = q V_{\text{accel}} \tag{3}$$

The acceleration potential, through which the ions fall, is approximately the discharge potential ($V_{\text{accel}} \sim V_d$). Therefore, the discharge voltage (nominally 300–500 V for a Hall thruster) must be reduced to reduce the exit velocity.

The difficulty of high-thrust-to-power operation is maintaining high levels of thrust efficiency when the propellant mass-flow rate increases and the discharge voltage decreases. Under high-thrust-to-power operation, desired power levels are in excess of 1 kW. Most of the research in the field of low-voltage Hall thrusters, however, focuses on reduced-power operation (low voltage and low current). For example, space qualified Hall thrusters, such as the Busek BHT-200, operate at relatively low voltages (250 V) but nominally at 200 W.‡ Alta created the XHT-100 Hall thruster by scaling their 1 kW thruster to design the main propulsion system for a micro- or minisatellite that operates nominally at 180 V and 100 W but with only 22% efficiency [2]. The Mitsubishi Electric Corporation reported performance results on their 200-mN-class Hall thruster of ~30% total thrust efficiency at ~200 V and ~1 kW [3]. In 2005 TsNIIMASH (Central Scientific Research Institute for Machine Building in Kaliningrad) reported ~45% efficiency for a thruster with anode layer operating at 200 V and 3.5 mg/s flow of xenon. They further demonstrated that the power and thrust can be linearly scaled with thruster arrays or clusters [4]. Clusters, however, add mass and complexity to the system that could be alleviated by a single thruster with identical capabilities. Literature is sparse for high powered Hall thrusters operating at low anode voltages (voltages less than 200 V and currents greater than 3 A). It is known that Hall thrusters do not perform well in this regime; however, the physics of the inefficiency and instability are unknown. In 2003, Manzella and Jacobson [5] experimented on the NASA-120M and NASA-457M Hall thrusters and identified voltage utilization efficiency as the leading loss mechanism of low-voltage operation. The devices in the

Presented as Paper 2008-4722 at the 44th AIAA/ASME/SAE/ASEE Joint Propulsion Conference & Exhibit, Hartford, CT, 21–23 July 2008; received 22 October 2009; accepted for publication 2 June 2010.

*Ph.D. Candidate, Student Member AIAA.
†Associate Professor. Member AIAA.

‡Data available online at http://busek.com/halleffect.html#low [retrieved 23 August 2010].

aforementioned study were operated as low as 100 V on the anode at less than 25% efficiency. Ashkenazy et al.'s [6] work found limited improvements by extending the discharge-chamber channel length. These improvements were only reported at low-power operation, however. Research in alternative propellants such as bismuth has been shown to lower the cost of ionization, a power loss aggravated at low discharge voltages [7,8]. Additionally, as a heavier atom than xenon, bismuth would also decrease the exit velocity for a given discharge voltage according to Eq. (3). Performance data for bismuth Hall thrusters are not yet available, however.

Using alternative propellants will benefit high-thrust-to-power operation but it does not address the physics inhibiting high efficiency. This is a parametric study of an Aerojet BPT-2000 Hall thruster operated at low voltages. By implementing a variety of thrust stand and probe studies the goal of this work was to better understand the underlying physics and diagnose as many loss mechanisms as possible. The probe study includes Faraday, emissive and retarding potential analyzer (RPA) probes to diagnose beam divergence, current efficiency, and voltage utilization efficiency.

II. Apparatus

All measurements were taken on an Aerojet BPT-2000 Hall thruster designed to operate nominally between 300 and 500 V [9]. The xenon testing facility is a 2-m-diam and 4-m-long vacuum chamber, where the thruster is mounted at the radial center 1 m from the end of the tank (see Fig. 1). Rough vacuum is reached by a 400 cfm two-stage rotary oil-sealed pump. High vacuum is reached and maintained by two 48 in. cryopumps that operate at $120,000$ liter/s (N_2). Chamber base pressure was 1×10^{-6} torr and the pressure did not exceed 4×10^{-5} torr (corrected for xenon) during thruster operation. Thrust measurements were taken by the use of an inverted-pendulum thrust stand [10]. The thrust stand is water-cooled to alleviate thermal drifts and its level is monitored by a tilt sensor accurate to one-half of an arcsecond. Anode and cathode propellant lines are controlled by thermal mass-flow controllers. The thrust stand was calibrated before each change in mass-flow rate. At each operating condition the magnets were adjusted to obtain the maximum thrust efficiency as calculated by thrust stand diagnostics. A laboratory-grade LaB_6 cathode was used for testing at a constant flow of 0.3 mg/s xenon. All efficiency values, both referenced and presented, exclude cathode flow and heater power.

Plume diagnostics were taken by three probes mounted on a three-axis motion table (rotational stage mounted upon two perpendicular linear slides. The Hall thruster was rigidly mounted in the tank (not on the thrust stand) for this portion of the tests and the probes were swept through the plume by the motion table.

Voltage utilization efficiencies were obtained by a four-grid RPA probe placed 0.55 m downstream from the thruster faceplate at 0, 15, and 30° to the thruster centerline. The RPA probe uses a series of biased grids to repel ions of low energy. Sweeping the retarding potential on the grids yields an ion-energy-per-charge distribution of the plume of the Hall thruster. The RPA grid wires are 0.114 mm in diameter with 0.140 mm spacing resulting in a 30% open area. Each grid is 0.254 cm from each other with the exception of the front floating grid which is 0.508 cm from the first electron repeller. The outer diameter of the grids is 1.235 cm and the outer diameter of the body of the probe is 3.170 cm. The electron repellers were biased 15 V below cathode. The ion repeller grid was swept from 0 V to 450 V for each trace. The current collected by the probe was then passed through a current amplifier and recorded by an oscilloscope. The anode and RPA were both referenced to cathode during data acquisition. In calculating the voltage utilization efficiency the repelling voltages were adjusted to be relative to ground potential and to account for the plasma potential.

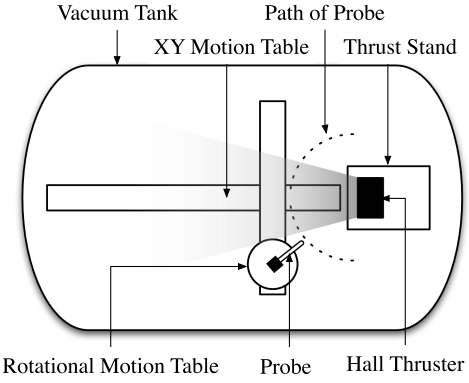

Fig. 1 Top-down view of the inside of the xenon Hall thruster testing facility.

Faraday probe sweeps yield ion current density measurements. Current density as a function of offaxis angle can then be used to compute beam divergence. The Faraday probe is enclosed in an alumina sheath with an outer diameter of 4.75 mm. A steel guard ring with a diameter of 10 mm was included to reduce edge effects on the potential structure in front of the probe face. The gap between the guard ring and collector face is 1.25 mm. Probe data were taken at 25 cm radius from the front plate of the thruster through a half-angle of 53° with an angular resolution of 2°.

Plasma potentials were recorded by an emissive probe constructed from a (1.27×10^{-4} mm diameter) thoriated tungsten wire encased in an alumina sheath and referenced to cathode potential. The potentials were recorded at 0, 15, and 30° 0.55 m downstream from thruster centerline (same as the RPA probe). Plasma potentials were extracted from the emissive probe traces using the intersection method discussed by Kemp and Sellen [11] in 1965 and first introduced by Langmuir [12] in 1923.

III. Efficiency Analysis

There are various loss mechanisms that degrade Hall thruster operation. As we will show, reducing the discharge voltage further aggravates many of these inefficiencies. Measurements from the thrust stand, mass-flow controllers, and discharge power supplies can be combined in real-time to produce thrust efficiency:

$$\eta_T = \frac{T^2}{2\dot{m}P_s} \tag{4}$$

Thrust efficiency is a measure of the discharge power conversion into net thrust of the system. A recast of the thrust efficiency equation breaks it into the product of energy efficiency, the measure of total energy in the ion beam, and propellant efficiency, the measure of the velocity distribution function and beam divergence efficiency [13]:

$$\eta_T = \frac{\frac{1}{2}\dot{m}\langle \mathbf{V}\rangle^2}{P_s} = \frac{\langle \mathbf{V}\rangle^2}{\langle \mathbf{V}^2\rangle}\frac{\frac{1}{2}\dot{m}\langle \mathbf{V}^2\rangle}{P_s} = \eta_p\eta_E \tag{5}$$

Energy efficiency can further be separated into voltage utilization efficiency and current efficiency, where the voltage utilization efficiency is the percentage of the anode–cathode potential that the ions are accelerated through and the current efficiency is the ratio of exhausted current to discharge current. Voltage utilization efficiency is expressed as

$$\eta_v = \frac{\frac{1}{2}m\langle \mathbf{V}^2\rangle}{eV_d}\frac{1}{f_i Q} \tag{6}$$

where $\frac{1}{2}m\langle \mathbf{V}^2\rangle = \langle \epsilon_{\text{ion}}\rangle$ and current efficiency is

$$\eta_c = \frac{\dot{m}e}{mI_d}(f_i Q) = \frac{I_i}{I_d} \tag{7}$$

where Q equals

$$Q = \frac{1}{f_i}(f_1 + 2f_2 + 3f_3)$$

The variable f_i is the ionization mass fraction of the propellant:

$$f_i = f_1 + f_2 + f_3 \ldots \qquad f_0 + f_i = 1$$

where f_0, f_1, f_2, and f_3 are the exit mass fractions of Xe, Xe^+, Xe^{2+}, and Xe^{3+}. Thus, thrust efficiency is the product of propellant, voltage utilization, and current efficiencies:

$$\eta_T = \eta_v \eta_c \eta_p \tag{8}$$

Voltage utilization efficiency can be measured with an RPA probe and the current efficiency can be obtained with Faraday probe data. An in-depth derivation of Eqs. (6) and (7) can be found in Larson et al.'s work [13].

The propellant efficiency is the product of the velocity distribution efficiency and the beam divergence efficiency [14]:

$$\eta_p = \frac{\langle |V| \rangle^2}{\langle |V|^2 \rangle} \langle \cos\beta \rangle^2 = \eta_{vdf} \eta_B \tag{9}$$

where β is the current-weighted average offaxis ion trajectory angle as determined by the Faraday probe, defined later in Eq. (11). The velocity distribution function can be measured with an ExB probe.

Finally, we can recast the thrust efficiency equation as the product of all four loss mechanisms:

$$\eta_T = \eta_v \eta_c \eta_{vdf} \eta_B \tag{10}$$

The term *thrust efficiency* has been used by Kim [1] but also appears under the name anode efficiency [15] and discharge efficiency [5] and refers to a benchmark for anode performance that excludes the magnets and cathode operation.

IV. Results

A. Thrust Stand

Figure 2 shows the thruster operated at above 50% thrust efficiency for all three mass-flow rates at 300 V. The data here are comparable with the data from [9] after accounting for the cathode operation for the 300 V data.[§] The discharge supply was current-limited to 6.6 A, eliminating the possibility of testing data for 4 mg/s discharge voltages below 140 V and below 180 V for 5 mg/s. At $V_d = 100$ V, maximum thrust efficiency was 15% for 3 mg/s.

The discharge current is the current that accumulates at the anode from ionization, secondary electron emission, and "recycled" electrons originating from the cathode. The discharge current is plotted against the discharge voltage in Fig. 3. The current levels were nearly constant for each mass-flow rate until the discharge voltage dropped below 200 V, where the current increased rapidly; again, this increase in current is the result of the magnetic field being optimized for maximum η_T.

B. Raw Probe Data

Figure 4 shows the current density as a function of angle for a flow rate of 3 mg/s. The measurements reflect the raw data as collected by the Faraday probe. As the discharge voltage is decreased the beam magnitude decreased at the center peak and increased in the higher offaxis angles. Facility limitations prohibited sweeps past 53°.

C. Derived Efficiencies

Current efficiency η_c is shown in Fig. 5, where I_d is measured directly from the discharge supply. The beam current I_i is obtained from an integration of $j(\theta)$ as measured by the Faraday probe. Current in the beam outside the probe's maximum offaxis angle of 53° was not collected, and therefore I_i is a lower bound. By using a linear extrapolation of the probe sweeps from 53 to 90° (assuming 0 A/m^2 at 90°) we estimate the amount of current that is omitted from our integration. This technique indicates our η_c calculations to have a maximum underestimation error of 12% due to the uncollected portions of the beam. Previous studies have shown, however, that the beam dies off much faster than linearly, and therefore our error is a conservative estimate. The efficiency decays linearly from 300–160 V and then begins to decline more rapidly.

[§]Data for discharge voltage lower than 300 V was not available for comparison.

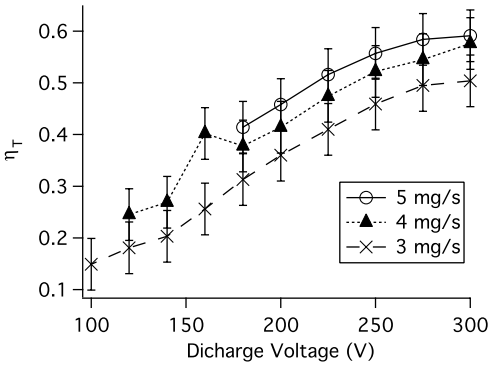

Fig. 2 Thrust efficiency as determined by thrust measurements. Error bars are calculated based on the reproducibility of calibration measurements both during operation and when the thruster is turned off.

The beam divergence efficiency, η_B in Fig. 6, was calculated using Faraday probe data and with the assumption that the plume was axisymmetric. The current values, $j(\theta)$, obtained by each trace create a weighted distribution function of the ion trajectory offaxis angles used to calculated the beam divergence efficiency:

$$\eta_B = \langle \cos\beta \rangle^2 = \left(\frac{\int \cos\theta j(\theta) r^2 \sin\theta \, \mathrm{d}\theta}{\int j(\theta) r^2 \sin\theta \, \mathrm{d}\theta} \right)^2 \tag{11}$$

Beam divergence efficiency is subject to underestimation based on the positioning of the Faraday probe and the assumption of

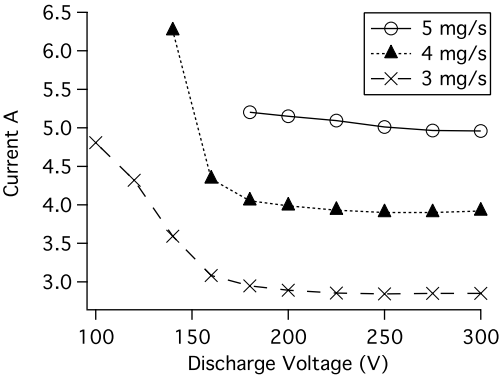

Fig. 3 Discharge current at maximum η_T. Uncertainty is ±0.05 A based on manufacturer's specified uncertainty for the discharge power supply.

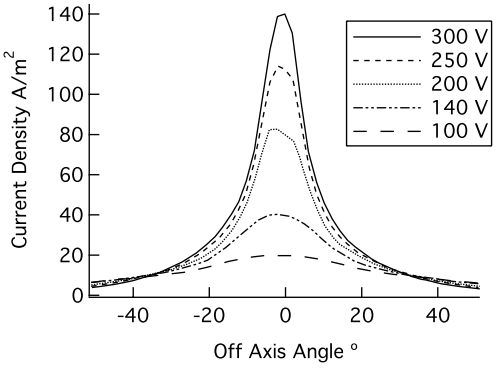

Fig. 4 Faraday probe sweeps 250 mm downstream for 3 mg/s flow rate at five different discharge voltages.

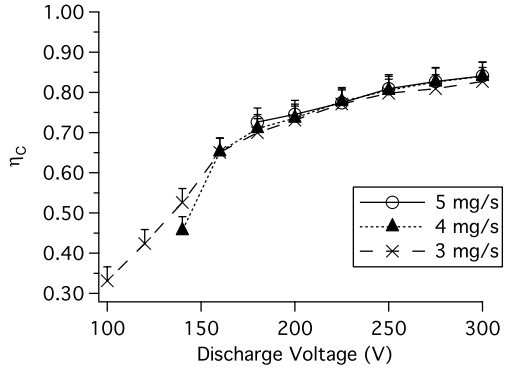

Fig. 5 Current efficiency as a function of discharge voltage.

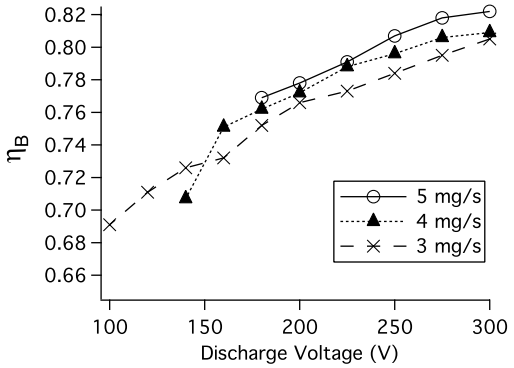

Fig. 6 Beam divergence efficiency as calculated by Eq. (11) from Faraday probe sweeps 250 mm downstream.

axisymmetry in the integral of Eq. (11). An accurate sweep would be positioned directly over the apex of the beam profile. If the probe is positioned off apex center it will result in a sweep that displays an artificially low beam current. By assuming a maximum vertical probe misalignment of $dx = 3$ cm, the maximum error in the calculation of η_B was estimated to be 3.5%. There is an unaccounted error due to the hemispherical integration of charge exchange ions at high angles, common to Faraday probe results [13].

Figures 7–9 display the integrated ion-energy-per-charge distributions for three offaxis angles. The greatest change in efficiency occurred in the 3 mg/s experiments where the voltage utilization efficiency dropped from 76% at 300 V to 54% at 100 V when the probe was positioned 30° offaxis. As seen with other Hall thrusters, the voltage utilization efficiency decreases with increasing offaxis angle [16]. The traces in Figs. 7–9 are referenced to cathode potential. Overall voltage utilization efficiency requires a reference correction with respect to ground and plasma potentials. Additionally, since the ion energy is function of offaxis angle, the calculation of a total voltage utilization efficiency must be properly weighted according to the current distribution function as obtained with the Faraday probe. These adjustments are outlined in Sec. V and are visible in Figs. 10–12. The dominant error in Figs. 7–9 came from the uncertainty in the integrated ion-energy-per-charge distributions due to noise in the recorded $\delta I/\delta V$ trace.

The ion-energy-per-charge distribution is dependent on the local plasma potential at the position of the probe. Even though the retarding grid is referenced to cathode, the energy the ions have acquired is equal to the potential drop between the discharge potential and the local plasma potential. In the absence of the probe, the ions will continue to accelerate until they reach their terminal potential, which, in the case of ground testing, is the tank wall (ground) potential. Hence, RPA measurements are sensitive to the location of the probe. Thus, to remove the positional dependence of the RPA, knowledge of both the local plasma potential and cathode to ground

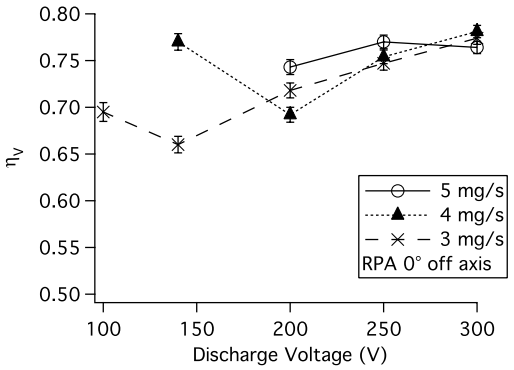

Fig. 7 $\bar{\epsilon}/eV_d$ as calculated from RPA data 0° offaxis and 550 mm downstream.

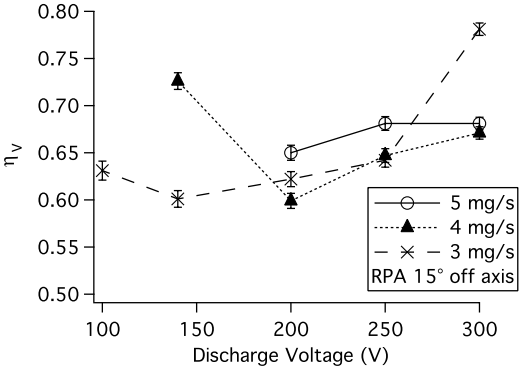

Fig. 8 $\bar{\epsilon}/eV_d$ as calculated from RPA data 15° offaxis and 550 mm downstream.

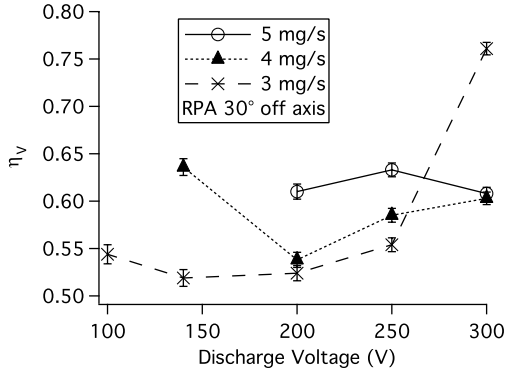

Fig. 9 $\bar{\epsilon}/eV_d$ as calculated from RPA data 30° offaxis and 550 mm downstream.

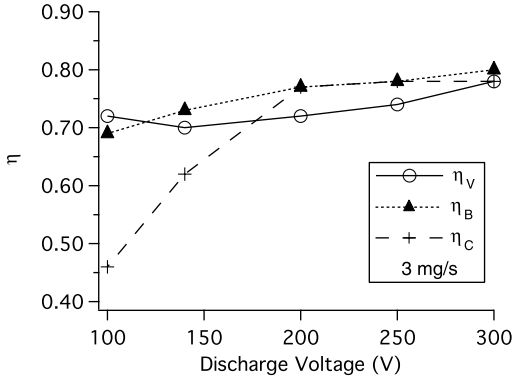

Fig. 10 η values for 3 mg/s.

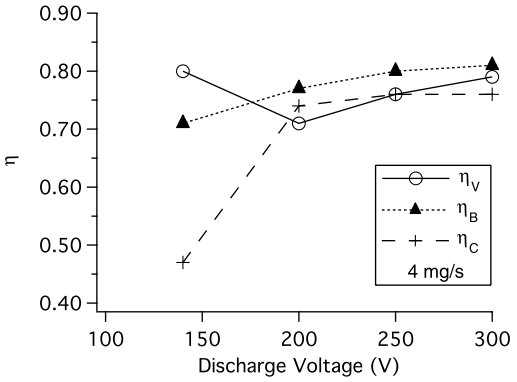

Fig. 11 η values for 4 mg/s.

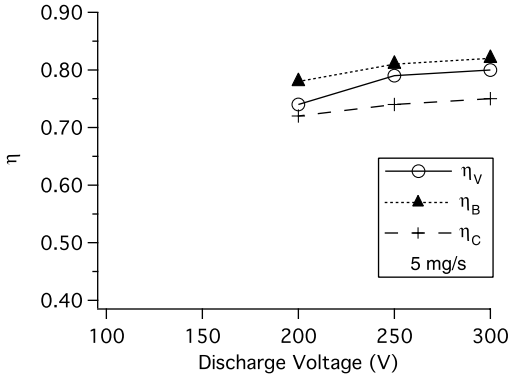

Fig. 12 η values for 5 mg/s.

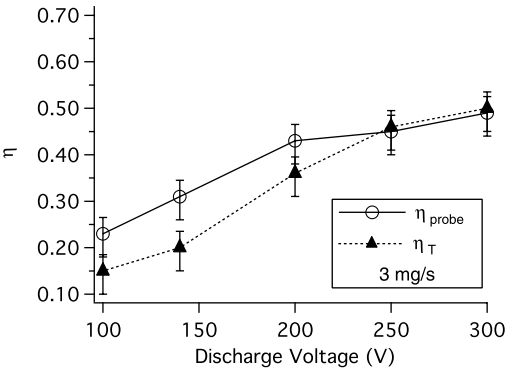

Fig. 13 Thrust efficiency from the thrust stand and probe efficiency from the probe studies for 3 mg/s.

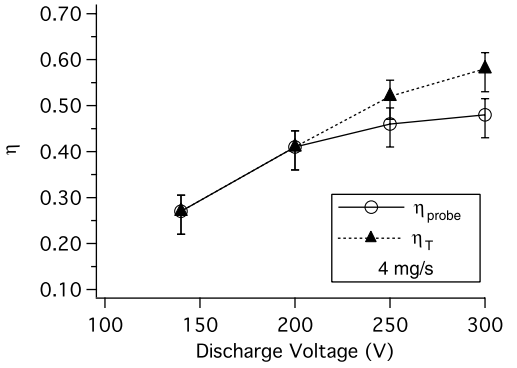

Fig. 14 Thrust efficiency from the thrust stand and probe efficiency from the probe studies for 4 mg/s.

potential is necessary. Assuming that the RPA grids are referenced to ground the energy values can be corrected by

$$\left\langle \frac{\epsilon_{\text{ion}}}{q} \right\rangle = \left\langle \frac{\epsilon_{\text{RPA}}}{q} \right\rangle - \Phi_{\text{ctg}} + \Phi_{\text{plasma}} \tag{12}$$

where the charge number is assumed to be unity and the left-hand side is the ion energy to be used in the correct calculation of Eq. (6).

RPA traces were taken at 0, 15, and 30° and average ion-energy values were linearly interpolated for angles in between 0 and 15° and in between 15 and 30°. The energy values from 30° out to 53° were assumed to be constant. While the validity of this extrapolation is admittedly unknown, past studies indicate the approach is reasonable. King's RPA results on a 1.5-kW-class Hall thruster showed that measured probe values varied less than 5% from 30 to 60° [16]. An assumption of 5% error in our high-angle extrapolated probe values propagates through the integral as 2% uncertainty in the calculation of Eq. (13). Finally, the traces are weighted against the current distribution function from the Faraday data and integrated to obtain the overall voltage utilization efficiency. Thus, by Eq. (13) the final values for η_V are obtained and are shown in Figs. 10–12:

$$\eta_V = \frac{\int \epsilon_{\text{ion}}(\theta) j(\theta) r^2 \sin\theta \, \mathrm{d}\theta}{qeV_d \int j(\theta) r^2 \sin\theta \, \mathrm{d}\theta} \tag{13}$$

V. Discussion

Figures 10–12 depict the various efficiency terms for each mass-flow rate as measured using probe techniques. The current efficiency becomes the dominant loss mechanism for all operation below 200 V. The voltage utilization efficiency increases with increasing mass-flow rate and with decreasing discharge potentials. Current and beam divergence efficiency, however, monotonically decay with decreasing discharge voltage. Experimentally, it is well known that η_c can be increased by adjusting the magnets to minimize the discharge current

Table 1 Comprehensive summary of all η values

Anode to cathode, V	Current, A	Mass flow, mg/s	Thrust, mN	Cathode to ground, V	Plasma to cathode, V	η_V	η_B	η_C	η_{probe}	η_T
300	2.85	3	65.63	−27.00	46.10	0.78	0.80	0.78	0.49	0.50
250	2.84	3	57.12	−26.30	41.85	0.74	0.78	0.78	0.45	0.46
200	2.89	3	45.62	−22.50	35.07	0.72	0.77	0.77	0.43	0.36
140	3.59	3	31.96	−13.90	18.53	0.70	0.73	0.62	0.31	0.20
100	4.81	3	26.77	−9.70	12.61	0.72	0.69	0.46	0.23	0.15
300	3.92	4	73.60	−28.10	49.88	0.79	0.81	0.76	0.48	0.58
250	3.90	4	63.82	−25.90	44.29	0.76	0.80	0.76	0.46	0.52
200	3.99	4	51.40	−24.60	37.65	0.71	0.77	0.74	0.41	0.41
140	6.26	4	43.44	−11.10	17.88	0.80	0.71	0.47	0.27	0.27
300	4.96	5	72.63	−28.70	54.32	0.80	0.82	0.75	0.49	0.59
250	5.01	5	64.71	−24.40	45.39	0.79	0.81	0.74	0.47	0.56
200	5.15	5	53.21	−23.90	41.28	0.74	0.78	0.72	0.42	0.46

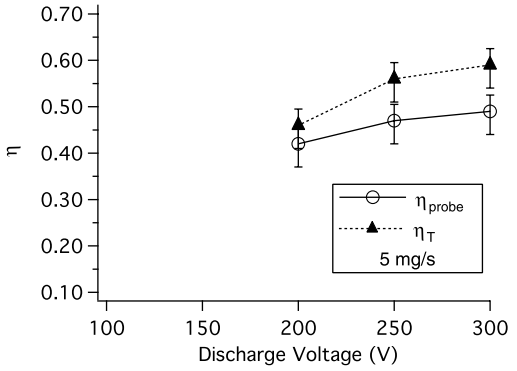

Fig. 15 Thrust efficiency from the thrust stand and probe efficiency from the probe studies for 5 mg/s.

[13]. In doing so, however, the thrust efficiency as a whole declined in spite of reduced discharge current. This implies that one of the remaining losses begins to penalize efficiency at a faster rate than the reduced anode current increased efficiency. Most unusual is the fact that the voltage utilization efficiency begins to increase at the lowest of discharge potentials. It may be that maximum thrust efficiency is obtained by maximizing voltage utilization and not current efficiency during operation at low discharge voltages.

Table 1 displays the final values for all calculated and experimentally determined loss mechanisms. Plasma-to-cathode values are displayed as determined by the emissive probe at 0.55 m downstream 0° offaxis. The probe studies measured three of the four loss mechanisms comprising thrust efficiency. The velocity distribution was not obtained, and therefore the probe efficiency is an upper bound on the thrust efficiency. Probe efficiency is defined as

$$\eta_{\text{probe}} = \eta_v \eta_c \eta_B = \frac{\eta_T}{\eta_{vdf}} \tag{14}$$

Figures 13–15 plot thrust and probe efficiencies as determined by the thrust stand and probe studies. The discrepancy between the probe and thrust stand values can be attributed to several things: overestimation of the beam divergence, inflated thrust measurements due to background neutrals, inflated thrust measurements due to cathode propellant ingestion, and underestimation of the current efficiency. The last of which is because the current fraction at high angles was not recorded. At low discharge voltages, where the beam divergence is greater this omission has a larger effect on the calculation of current efficiency. The two benchmarks are in closest alignment at low discharge voltages for the 4 and 5 mg/s trials, and in the highest of discharge voltages for the 3 mg/s trial.

VI. Conclusions

Probe studies and thrust stand measurements were performed on an Aerojet BPT-2000 Hall thruster at discharge voltage from 100 to 300 V for 3 to 5 mg/s flow of xenon. The Hall thruster was unable to run stably at discharge voltages below 180 V at 5 mg/s. Thrust efficiencies determined by the thrust stand measurements reached as low as 15% and the probe studies recorded as low as 23%. The dominant loss mechanism at the lowest discharge potentials was the current efficiency, whereas the voltage utilization efficiency increased in value; the only loss mechanism to do so across all operating conditions. While the current efficiency can be increased by adjusting the magnet current, overall thrust efficiency suffers, indicating a coupled effect with one of the other loss mechanisms.

References

[1] Kim, V., "Main Physical Features and Processes Determining the Performace of Stationary Plasma Thrusters," *Journal of Propulsion and Power*, Vol. 14, No. 5, 1998, pp. 736–743. doi:10.2514/2.5335

[2] Andrenucci, M., Berti, M., Biagioni, L., and Cesari, U., "Characteristics of the XHT-100 Low Power Hall Thruster Prototype," *4th International Spacecraft Propulsion Conference*, ESA SP-555, Paris, Oct. 2004.

[3] Ozaki, T., Inanaga, Y., Nakagawa, T., and Osuga, H., "Development Status of 200 mN Class Xenon Hall Thruster of MELCO," 29th International Electric Propulsion Conference, IEPC Paper 2005-064, Princeton, NJ, 2005.

[4] Zakharenkov, L. E., Semenkin, A. V., and Garkusha, V. I., "Study of the 3-TAL Thruster Assembly Operation," 29th International Electric Propulsion Conference, IEPC Paper 2005-185, Princeton, NJ, 2005.

[5] Manzella, D., and Jacobson, D., "Investigation of Low-Voltage/High-Thrust Hall Thruster Operation," 39th AIAA/ASME/SAE/ASEE Joint Propulsion Conference and Exhibit, AIAA Paper 2003-5004, Huntsville, AL, July 2003.

[6] Ashkenazy, J., Shitrit, S., and Appelbaum, G., "Hall Thruster Modifications for Reduced Power Operation," 29th International Electric Propulsion Conference, IEPC Paper 2005-080, Princeton, NJ, 2005.

[7] Massey, D. R., King, L. B., and Makela, J. M., "Progress on the Development of a Direct Evaporation Bismuth Hall Thruster," 29th International Electric Propulsion Conference, IEPC Paper 2005-256, Princeton, NJ, 2005.

[8] Kieckhafer, A., and King, L. B., "Energetics of Propellant Options for High-Power Hall Thrusters," 41st AIAA/ASME/SAE/ASEE Joint Propulsion Conference and Exhibit, AIAA Paper 2005-4228, Tucson, AZ, July 2005.

[9] King, D., Tilley, D., Aadland, R., Nottingham, K., Smith, R., Roberts, C., Hruby, V., Pote, B., and Monheiser, J., "Development of the BPT Family of U.S.-Designed Hall Current Thrusters for Commercial LEO and GEO Applications," 34th AIAA/ASME/SAE/ASEE Joint Propulsion Conference and Exhibit, AIAA Paper 1998-3338, Cleveland, OH, July 1998.

[10] Haag, T. W., "Design of a Thrust Stand for High Power Electric Propulsion Devices," 25th AIAA/ASME/SAE/ASEE Joint Propulsion Conference & Exhibit, AIAA Paper 1989-2829, Monterey, CA, July 1989.

[11] Kemp, R. F., and Sellen, J. M., Jr., "Plasma Potential Measurements by Electron Emissive Probes," *Review of Scientific Instruments*, Vol. 37, No. 4, 1966, pp. 455–461. doi:10.1063/1.1720213

[12] Langmuir, I., *The Collected Works of Irving Langmuir*, Vol. 5, edited by C. Guy Suits, Pergamon, New York, 1961, pp. 1–10.

[13] Larson, C. W., Brown, D. L., and Hargus, W. A., "Thrust Efficiency, Energy Efficiency, and the Role of the VDF in Hall Thruster Performance Analysis," 43rd AIAA/ASME/SAE/ASEE Joint Propulsion Conference and Exhibit, AIAA Paper 2007-5270, Cincinnati, OH, July 2007.

[14] Bugrova, A. I., Kim, V., Maslennikov, N. A., and Morozov, A. I., "Physical Processes and Characteristics of Stationary Plasma Thrusters With Closed Electrons Drift," *AIDAA/AIAA/DGLR/JSASS 22nd International Electric Propulsion Conference*, Viareggio, Italy, Oct. 1991.

[15] Hofer, R. R., and Gallimore, A. D., "Efficiency Analysis of a High-Specific Impulse Hall Thruster," 40th AIAA/ASME/SAE/ASEE Joint Propulsion Conference & Exhibit, AIAA Paper 2004-3602, Ft. Lauderdale, FL, July 2004.

[16] King, L. B., "Transport-Property and Mass Spectral Measurements in the Plasma Exhaust Plume of a Hall-Effect Space Propulsion System," Ph.D. Thesis, Univ. of Michigan, Ann Arbor, MI, 1998.

A. Gallimore
Associate Editor